








Carbon Stock Estimation Using the InVEST Model in Pante Ceureumen Protected Forest, West Aceh, Indonesia (2016–2025)

Siti Nurhaliza¹, Ichwana Ramli^{1,2*}, Ashabul Anhar³, Ashfa Achmad⁴, Jumadil Akhir⁵

¹ Master Program of Environmental Management, Graduate School, Syiah Kuala University, Banda Aceh 23111, Indonesia

² Department of Agricultural Engineering, Faculty of Agriculture, Syiah Kuala University, Banda Aceh 23111, Indonesia

³ Department of Forestry, Faculty of Agriculture, Research Center for Forestry and Ecosystem, Syiah Kuala University, Banda Aceh 23111, Indonesia

⁴ Department of Architecture and Planning, Faculty of Engineering, Syiah Kuala University, Banda Aceh 23111, Indonesia

⁵ Department of Forestry, Faculty of Agriculture, Syiah Kuala University, Banda Aceh 23111, Indonesia

Corresponding Author Email: ichwana.ramli@usk.ac.id

Copyright: ©2026 The authors. This article is published by IETA and is licensed under the CC BY 4.0 license (<http://creativecommons.org/licenses/by/4.0/>).

<https://doi.org/10.18280/ijdne.210505>

ABSTRACT

Received: 16 March 2026

Revised: 15 May 2026

Accepted: 25 May 2026

Available online: 31 May 2026

Keywords:

carbon stock, land use change, InVEST model, Sentinel-2 imagery, land cover, forest ecosystem, classification accuracy, kappa coefficient

Land use change is a major factor that influencing the dynamics of carbon stocks in forest ecosystems. An analysis was conducted on the Pante Ceureumen Protected Forest for the 2016-2025 period using 10m resolution Sentinel-2 imagery, supervised Maximum Likelihood Classification (MLC), a confusion matrix accuracy test based on 50 sample points, and InVEST modeling. The classification yielded 11 land cover classes with an overall accuracy score of 86% and a Kappa coefficient of 82.78%, indicating a high level of precision. Carbon stock estimation using aboveground and belowground carbon components based on the Ministry of Environment and Forestry (KLHK) carbon density values showed a decrease of 2,543,190.12 Mg C, from 11,850,478.20 Mg C in 2016 to 9,307,288.08 Mg C in 2025. This decline is influenced by a loss in the area of primary forest by 2,613.37 ha and secondary forest by 6,815.91 ha due to conversion to scrubland, mixed agriculture, and mining.

1. INTRODUCTION

Carbon stocks are one of the key indicators in the ecosystem services assessment due to their ability to reflect the productive capacity and ecological resilience of terrestrial ecosystems in response to change [1, 2]. Increasing land use utilisation is a key component of land-use change dynamics; it has been identified as a major factor contributing to the decline in the quality and functions of ecosystem services [3, 4].

Land use change, forest and soil degradation, and deforestation are major factors contributing to increased greenhouse gas emissions [5]. Over the past 150 years, land cover change caused by human activities has contributed approximately one-third of total global CO₂ emissions [6-9]. However, the magnitude of net carbon fluxes remains subject to significant uncertainty, primarily due to limitations in estimating terrestrial carbon density as well as the dynamics of global afforestation and deforestation rates [7].

Traditional field-based inventory methods are often impractical for monitoring biomass over large areas because they require substantial time and effort. Consequently, the integration of remote sensing data with sample plot measurements has become a widely adopted approach for estimating forest aboveground biomass [10, 11].

Carbon density methods based on land use type and estimation of vegetation indices are commonly used as empirical models. However, empirical models have

limitations because they require a large number of observational samples, which can increase uncertainty in simulation results. Contrary with that fact, remote sensing-based simulation models utilize land cover and vegetation information and offer the advantages of wide geographic coverage, easy data access, and no need for field sampling [12]. Some of the remote sensing models commonly used in carbon stock simulations include CASA, GLO-PEM, and CEVSA [13-15]. However, these models demand a high level of accuracy on land use data and vegetation cover in the research area.

Integrated Valuation of Ecosystem Services and Trade-offs (InVEST) is a widely used ecosystem modeling tool for evaluating ecosystem services, particularly for estimating and projecting a region's carbon stocks [16]. The carbon stock analysis in this model can track changes in carbon stock over time using a relatively simple approach that does not require complex parameters or advanced technical expertise [17]. Various studies indicate that this model has been widely applied in a variety of research contexts. As an example, research [18] evaluates the relationship between land-use change and carbon stock dynamics in the Loess Plateau, China. Meanwhile, the spatial-temporal distribution patterns of carbon stock in Shanxi Province indicate that socioeconomic factors play a greater role than biophysical factors in influencing variations in carbon stocks [19].

The strength of this model lies in its integration with

geographic information systems (GIS), enabling it to display detailed distributions of carbon stocks and support natural resource management policies based on scientific data. Additionally, the InVEST model is spatially explicit, using maps to visualize the locations where ecosystem services are provided and utilized. This tool is designed to be simple, fast, and easily adaptable to data availability and decision-making contexts [20].

Global trends in forest carbon sequestration research indicate that much of the attention has been focused on the carbon sequestration potential of tropical forests and secondary forests, as well as total carbon stocks within ecosystems, including litter components. Previous studies indicate that research in this field continues to undergo significant development. Therefore, this study is expected to contribute to the body of knowledge regarding forest carbon sequestration. Some of the key contributors to this research include the United States, China, and Canada [21].

The Pante Ceureumen Protected Forest in Aceh Barat Regency is a vital component of the tropical forest ecosystem, serving as a carbon sink, a regulator of the water cycle, and a pillar of regional environmental balance. Despite its high ecological value, this area faces increasing anthropogenic pressures due to land use conversion, illegal mining activities, agricultural land clearing, plantation expansion, and weak forest governance. These activities lead to reduced forest cover and increased fragmentation of the area, which directly impacts carbon storage capacity. This situation is a critical concern because changes in land cover within protected forest areas not only affect local environmental quality but also contribute to increased carbon emissions and climate change. This Pante Ceureumen Protected Forest Area is important to

be studied because, in recent years, this region has experienced.

Various studies have used Sentinel-2 imagery and the InVEST model to estimate carbon stocks, but the application of these methods to the Pante Ceureumen Protected Forest, which faces pressure from illegal mining and land-use conversion, remains rare. This study provides the latest information on changes in carbon stocks from 2016 to 2025 in the protected forest area in West Aceh through the integration of Sentinel-2 imagery and the InVEST model.

2. RESEARCH METHODOLOGY

2.1 Research location

This study was conducted in the protected forest area of Pante Ceureumen, Aceh Barat. The research was carried out in February 2026. The study area covers 35,122.82 hectares. Geographically, the research location is located at 4°32'30" N and 96°20'0" E. The area has an elevation range of 20 to over 1,500 meters above sea level, with a topography dominated by hills and mountains. Based on its climatological characteristics, the study area has a tropical climate typical of the southwestern coastal region of Aceh. The dominant forest ecosystem type in the study area is dryland tropical rainforest. The forest area boundaries are based on official data from the National Geospatial Information Agency (BIG) and forest area maps from the Ministry of Environment and Forestry (KLHK). These biophysical conditions influence vegetation distribution and carbon storage capacity within the study area. The location of the study area is presented in Figure 1.

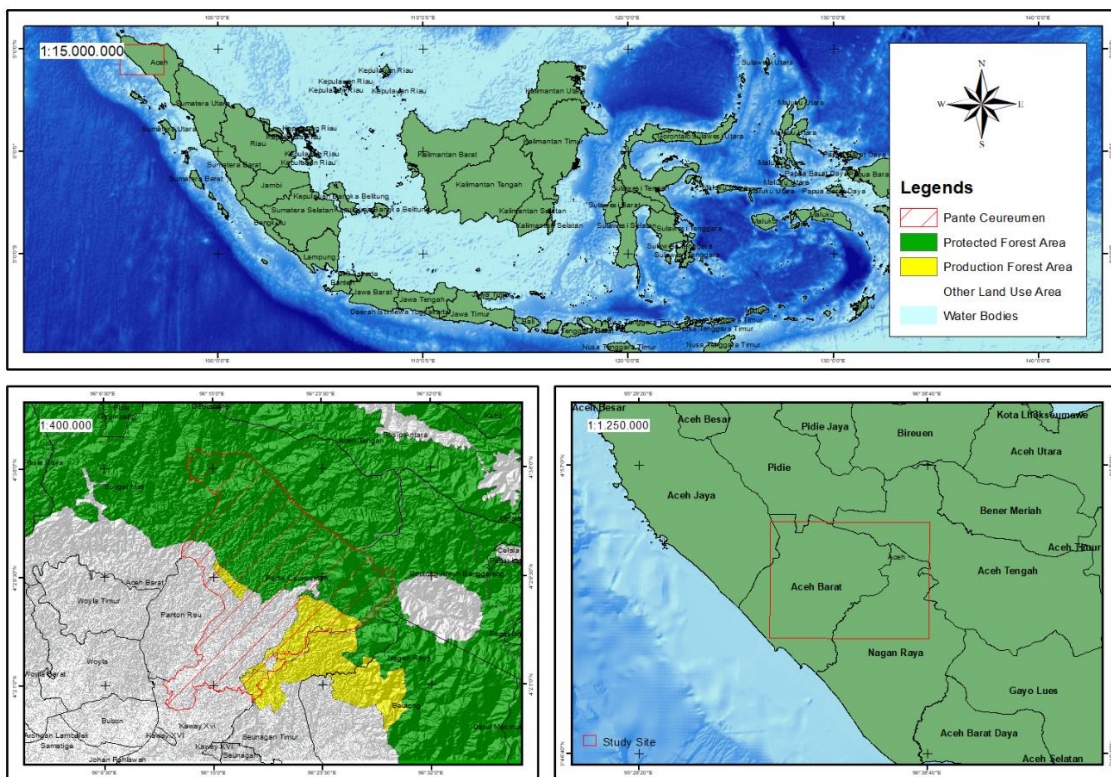


Figure 1. Research location

This study uses a secondary data obtained through literature reviews and the collection of spatial data from various sources.

The data used includes Sentinel-2 Level-2A satellite imagery with a spatial resolution of 10 meters, as well as boundary and

location data sourced from the National Geospatial Information Agency (BIG). Data processing and analysis were conducted using ArcGIS and InVEST software. The satellite imagery analyzed covers the years 2016 and 2025.

2.2 Data analysis

In this study, the method used to determine carbon stock estimates is the InVEST model, developed by the *Natural Capital Project*. Land cover classification of Sentinel-2 imagery from 2016 to 2025 was performed using supervised classification with the Maximum Likelihood Classification (MLC) algorithm. The MLC algorithm was used to group pixels into land cover class based on the highest statistical probability value for each class, as determined by the training data. The classification process was performed using ArcGIS software.

2.2.1 Accuracy test classification

Confusion matrix-based accuracy tests were used to assess the agreement between land cover classification results and reference data. Accuracy parameters were derived from this matrix. Overall Accuracy (OA) indicates the proportion of correctly classified pixels relative to the total sample, while the Kappa Coefficient is used to measure the level of agreement while accounting for the probability of random agreement. The Kappa coefficient was first introduced by Cohen in 1960. This coefficient is expressed in the form of a confusion matrix to measure the agreement between classification results and reference data [22].

Sample points for the accuracy test were selected using a stratified random sampling method based on the land cover classes resulting from the classification. A total of 50 sample points were used and distributed proportionally across each land cover class to represent the spatial conditions of the study area. Sample points were determined randomly within each land cover class and then verified through visual interpretation using a high-resolution image basemap in ArcGIS as well as ground checks. The accuracy test was conducted on the 2025 classification results because high-resolution reference and visual verification data were more adequate for that period, while the 2016 classification was used as comparative temporal data.

$$\text{Overall Accuracy} = \frac{\sum_i X_{ii}}{N}$$

where,

- X_{ii} : Number of pixels classified into class- i
- r : Number of classes
- N : Number of overall pixel

$$\text{Kappa Coefficient} = \frac{N \sum_{i=1}^r X_{ii} - \sum_{i=1}^r (X_{i+} \cdot X_{+i})}{N^2 - \sum_{i=1}^r (X_{i+} \cdot X_{+i})}$$

where,

- X_{ii} : Number of pixels correct on class- i
- X_{i+} : Number of i -throw Jumlah baris ke- i
- X_{+i} : Number of i -column
- r : Number of classes
- N : Number of overall pixel

2.2.2 Carbon stocking using the InVEST model

The formula for calculating total carbon stocks using the InVEST model is as follows [23].

$$C_j = C_a + C_b + C_s + C_d$$

where,

- C_j : Total carbon density
- C_a : Aboveground carbon
- C_b : Belowground carbon
- C_s : Soil carbon
- C_d : Dead organic matter

$$C_t = \sum_{j=1}^n C_j \times A_j, (j = 1, 2, \dots, n)$$

where,

- C_t : Number of stock carbon in ecosystem (ton)
- C_j : Carbon density on j -th land use class (ton/ha)
- A_j : Total area of j -th land use class (ha)
- n : Number of land use class

The carbon density values for each land cover class in this study, as calculated using the InVEST model, include only aboveground carbon and belowground carbon. Soil carbon and dead organic matter were not included in the analysis due to the limited availability of suitable data for the study area. The carbon stock values refer to the document National Forest Reference Level for Deforestation, Forest Degradation and Enhancement of Forest Carbon Stock, published by the KLHK of the Republic of Indonesia.

According to the classification by the KLHK of the Republic of Indonesia, the "mixed dryland farming" class refers to dryland agricultural areas interspersed with shrubs, thickets, and logged-over forests. Carbon storage in this class is assumed to be at a moderate level, meaning lower than in forested areas but higher than in open land or settlements. The carbon density values used as input in the InVEST model for each land use and land cover class are presented in Table 1.

Table 1. Carbon density value according to land use classes (model InVEST input)

Land Use and Land Cover	Aboveground Carbon (Mg C ha ⁻¹)	Belowground Carbon (Mg C ha ⁻¹)
Water body	0	0
Shrubs	60.39	14.25
Primary dryland forest	340.72	98.81
Secondary dryland forest	221.45	64.22
Mixed dryland farming	64.64	12.93
Plantation	48.1	15.63
Settlement	2.17	0.63
Dryland agriculture	14.08	2.82
Ricefield	10	2.36
Open land	2.4	0.57
Mines	0	0

Classification errors in certain land cover classes, particularly those with similar spectral characteristics such as dryland agriculture mixed with shrubs and thickets, can affect the results of carbon stock estimates. The similarity in spectral responses among vegetation classes in Sentinel-2 imagery makes it difficult to optimally distinguish some pixels, especially in areas with mixed vegetation cover and varying levels of density. Inaccuracies in land cover class identification can lead to discrepancies in area estimates, thereby affecting carbon stock calculations using the InVEST model. However, an overall accuracy of 86% and a Kappa coefficient of 82.78% indicate that the classification results possess a good level of precision and are suitable for use in carbon stock analysis.

3. RESULT AND DISCUSSION

3.1 Land use and land cover data analysis and processing

The use of Level-2A satellite imagery, such as Sentinel-2, in land cover analysis enables the identification of temporal changes through time-series comparisons. This technique is widely used in research in Indonesia because it can detect changes in vegetation and land-use conversion. Furthermore, with appropriate classification methods and accuracy tests, satellite imagery can achieve a high level of precision in land cover mapping.

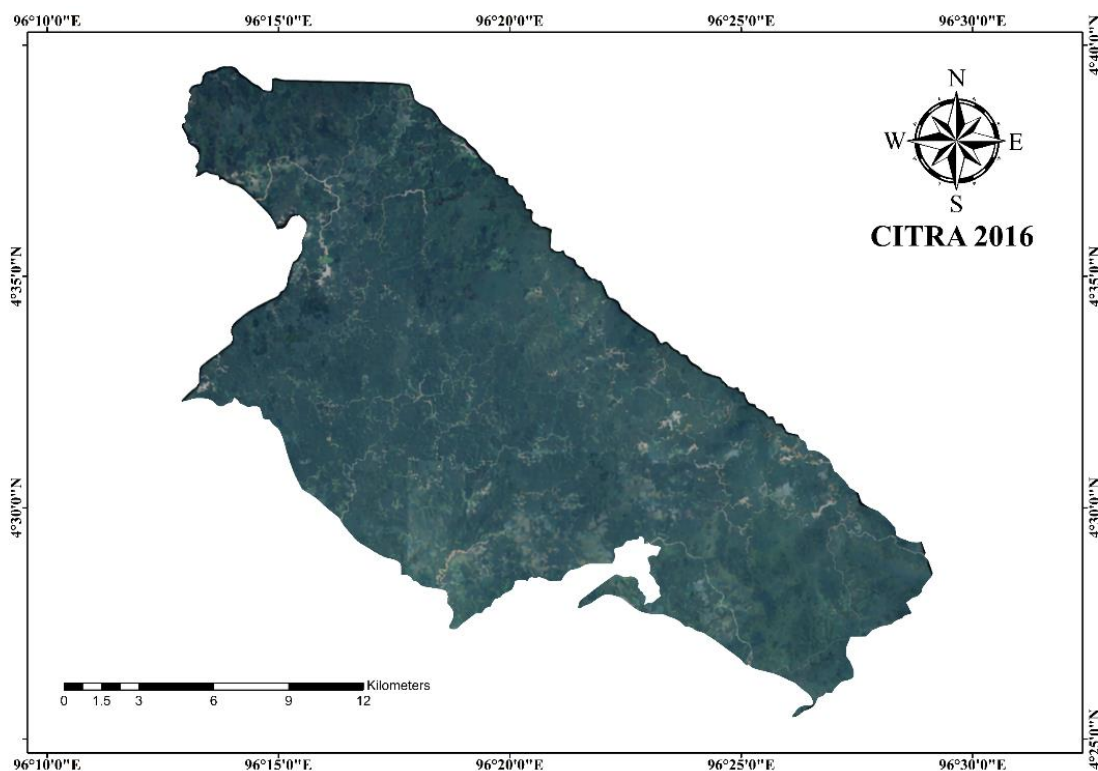
Based on the images derived from the interpretation of satellite imagery from 2016 and 2025 in the Pante Ceureumen Protected Forest, there are significant differences in land cover conditions. In 2016, land cover was dominated by forest vegetation that was still dense and relatively homogeneous, as indicated by darker hues and a uniform texture. These conditions suggest that during that period, the protected forest area was still in relatively good condition with a low level of disturbance. The Sentinel-2 imagery used in this study is

shown in Figure 2.

By 2025, changes in land cover patterns are evident, marked by the emergence of lighter-colored areas and more varied textures. These changes indicate the presence of illegal mining activities, which have led to intensive land clearing and the loss of vegetation cover. These activities have resulted in a decrease in vegetation density and changes in land surface characteristics. Changes in land use and land cover are the primary consequences of forest degradation [24, 25]. In addition, the appearance of linear patterns in the imagery indicates the presence of access roads or distribution routes for mining products that were constructed to support illegal mining activities, which indirectly contribute to the disruption of the integrity of the Pante Ceureumen Protected Forest, Aceh Barat. Based on the results of the image interpretation, further analysis was conducted through a land cover classification process to obtain more detailed and quantifiable information, as presented in Figure 3.

The results of land cover classification for 2016 and 2025 in the Protected Forest area of Pante Ceureumen Subdistrict indicate significant spatial changes. In 2016, land cover was still dominated by forest classes—both primary and secondary forests—which appeared to merge and form relatively intact blocks. Vegetation distribution during this period tended to be homogeneous, with land disturbances still limited to specific areas, particularly in the southern region. This indicates that, in that year, the forest ecosystem remained relatively stable and had not yet faced intense pressure.

On the contrary, by 2025, a more complex and fragmented pattern of land cover is evident. Previously extensive and contiguous forest areas are beginning to fragment into smaller patches, accompanied by an increase in the extent of non-forest land uses such as agriculture, plantations, settlements, and open land. These changes are particularly evident in the central to southern parts of the study area, which show higher levels of human activity.



11 July 2016

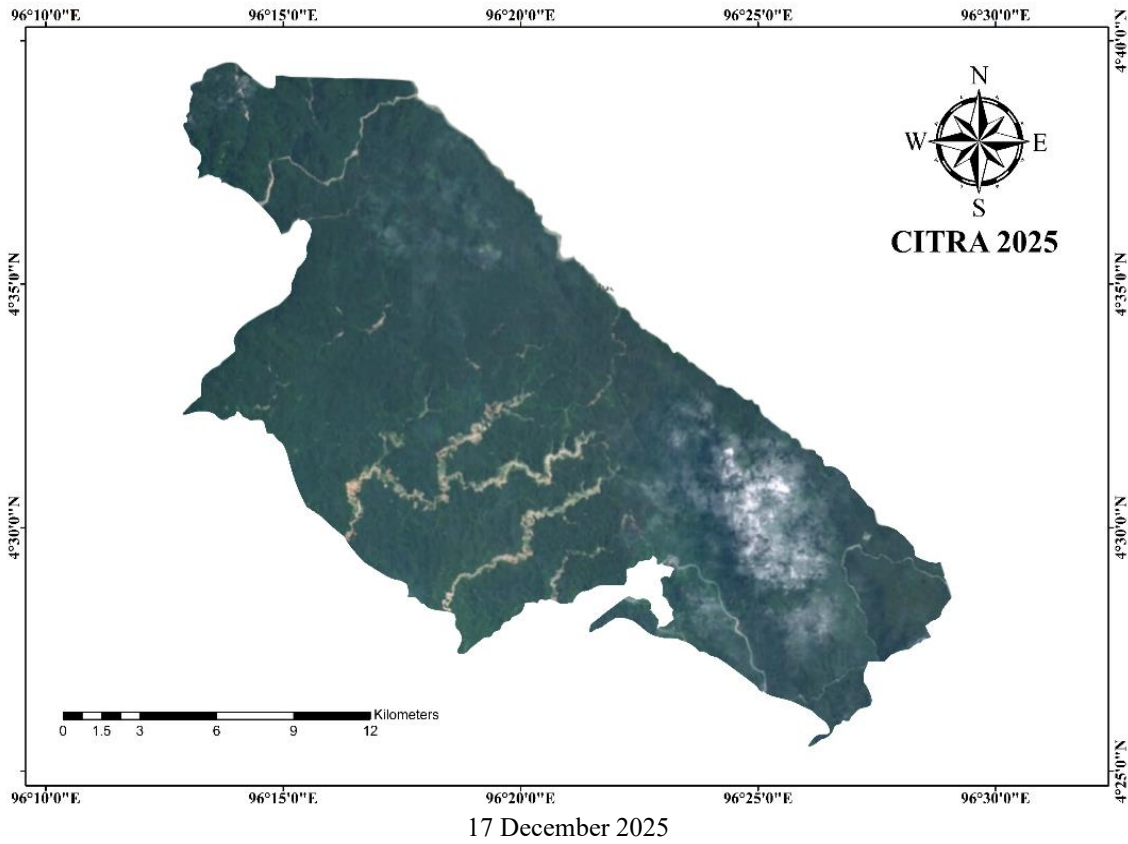
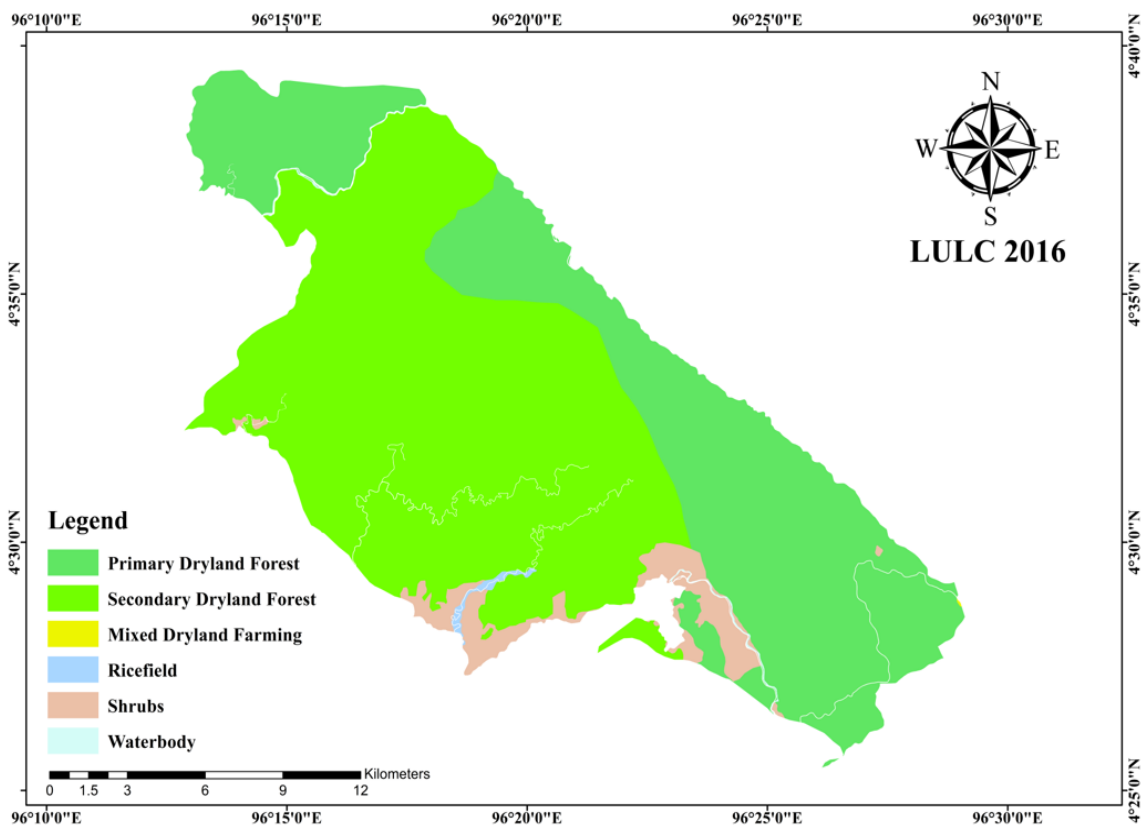


Figure 2. Sentinel-2 imagery on Pante Ceureumen Protected Forest



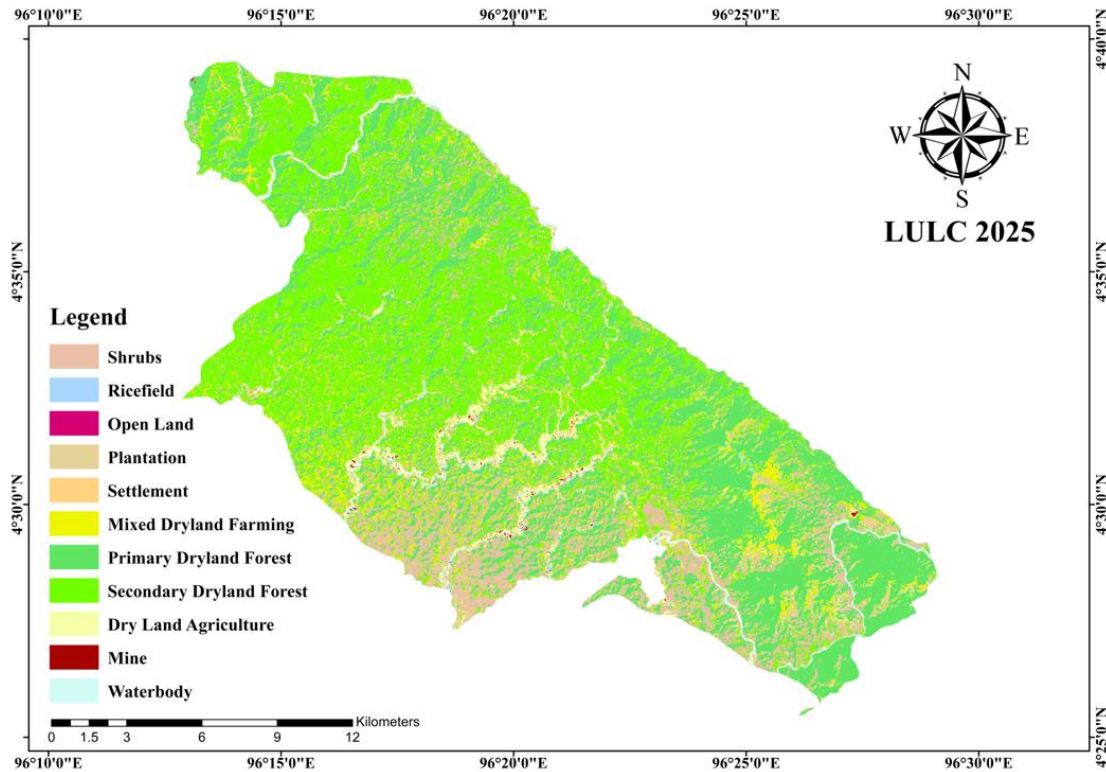


Figure 3. Land cover classification in 2016 and 2025

Deforestation and the loss of forest cover are major factors contributing to rising carbon emissions, particularly in developing countries. The loss of forest cover leads to the release of stored carbon into the atmosphere while simultaneously reducing future carbon sequestration potential. This situation underscores the importance of implementing policies and guidelines that support sustainable forest management and reforestation [26, 27].

Mining activities in the Xuzhou region have contributed to a decline in vegetation carbon stocks, as indicated by remote sensing data [28]. On the other hand, land-use changes in Shanxi Province (1990–2020), particularly the conversion of agricultural land and grasslands into mining and construction areas, were the primary factors driving the decline in carbon stocks, despite increases in forested land and built-up areas [29].

3.2 Land use and land cover change

An analysis of land use and land cover changes in the Protected Forest area of Pante Ceureumen Subdistrict reveals significant shifts in the extent of each land cover class during the 2016–2025 period. Details regarding the magnitude of these changes are presented in Table 2.

Based on Table 2, changes in land use and land cover in the Protected Forest area of Pante Ceureumen Subdistrict during the 2016–2025 period indicate a significant shift from forest to non-forest land. The area of primary dryland forest decreased from 14,157.89 ha (40.31%) to 11,544.52 ha (32.87%), while the area of secondary dryland forest also decreased from 19,326.28 ha (55.02%) to 12,510.37 ha (35.62%).

Furthermore, there was a significant increase in the non-forest category, specifically the shrubland category, which rose significantly from 1,483.92 ha (4.22%) to 5,280.13 ha (15.03%), indicating a process of forest cover degradation into

lower-quality secondary vegetation. Additionally, the emergence of land-use classes such as plantations, dryland agriculture, and mixed dryland agriculture with shrubland indicates the conversion of forest land into cultivated land, which can be identified through land-cover change analysis using satellite imagery. Other changes are also evident in the emergence of settlement and mining areas that were not previously identified in 2016. This indicates an increase in human activity within the protected forest area, which contributes to the reduction in forest cover.

Table 2. Land use change dynamics

Land Use	2016	%	2025	%
Primary dryland forest	14,157.8	40.3	11,544.5	32.8
Secondary dryland forest	19,326.2	55.0	12,510.3	35.6
Open land	0.00	0.00	2.56	0.01
Plantation	0.00	0.00	1,287.46	3.67
Settlement	0.00	0.00	88.34	0.25
Dryland agriculture	0.00	0.00	1,148.56	3.27
Mixed dryland farming	2.14	0.01	2,721.58	7.75
Ricefield	87.52	0.25	208.09	0.59
Shrubs	1,483.92	4.22	5,280.13	15.0
Mine	0.00	0.00	43.43	0.12
Waterbody	65.07	0.19	287.80	0.82
Total	35,122.8	100	35,122.8	100

3.3 Accuracy assessment

The accuracy test was conducted using the error matrix method based on ground-truth data collected from 50 sample points. Of these points, 43 matched the image classification results, while 7 did not.

Table 3. Accuracy assessment

Land Use and Land Cover 2025	Primary Dryland Forest	Secondary Dryland Forest	Open Land	Plantation	Settlement	Dryland Agriculture	Mixed Dryland Farming	Rice Field	Shrubs	Mine	Water Body	T	User Accuracy %
Primary dryland forest	12	1						1				1	85.71%
Secondary dryland forest	1	13						1				4	86.67%
Open land			1									5	100%
Plantation				2								2	100%
Settlement					1							1	100%
Dryland agriculture						2						2	100%
Mixed dryland farming						1	3					4	75%
Ricefield								1				1	100%
Shrubs							2		5			7	71.43%
Mine										1		1	100%
Waterbody											2	2	100%
Total	13	14	1	2	1	3	5	3	5	1	2	50	
Producer accuracy %	92.31%	92.86%	100%	100%	100%	66.67%	60%	33.33%	100%	100%	100%		
Overall accuracy %						86.00%							
Kappa accuracy %						82.78%							

Note: T: Total

The accuracy assessment in Table 3 shows that the overall accuracy reached 86%, and the Kappa coefficient was 82.78%. These values indicate a high level of agreement between the classification results and field conditions, meaning that the resulting land cover map is sufficiently accurate and can represent actual conditions on the ground. A Kappa value of 82.78% falls into the “near-perfect” category according to the classification [30].

Data quality in this study was achieved through several stages, namely the use of geometrically and atmospherically corrected Sentinel-2 Level-2A imagery, the land cover classification process using the MLC method, and accuracy testing using a confusion matrix based on 50 sample points from visual interpretation and ground checks. The accuracy test results showed an overall accuracy of 86% and a Kappa coefficient of 82.78%, indicating that the classification results have a high level of precision and are suitable for use in carbon stock analysis. Additionally, the carbon stock values used were derived from secondary data referencing the National Forest Reference Level for Deforestation, Forest Degradation, and Enhancement of Forest Carbon Stock, making them relevant to the characteristics of Indonesia’s tropical forest ecosystems.

3.4 Carbon stock estimation using the InVEST model

This study utilizes the InVEST model to estimate changes in carbon stocks over the 2016–2025 period. The InVEST model integrates two main components: aboveground carbon and belowground carbon. Carbon stock estimates were derived using carbon density data for each land cover type, which were then overlaid with raster land cover data to obtain information on total carbon stocks and their spatial distribution. All of the carbon stock estimation in this study is expressed in megagrams of Carbon (Mg C), which is numerically equivalent to tons of carbon (tons C). The results of the carbon stock calculations using the InVEST software are presented in Tables 4 and 5.

According to Table 4, the total carbon stock in the Pante Ceureumen Protected Forest area in 2016 was recorded at 11,850,478.2. This figure indicates that, under initial conditions, the land cover dominated by primary and secondary dryland forest made a very significant contribution to the area’s total carbon stock.

Table 4. Carbon stock changed according to land use in 2016

2016			
Land Use and Land Cover	Area	Carbon Density	Total (Mg C)
Secondary dryland forest	19,326.28	509.15	5,507,508.9
Primary dryland forest	14,150.38	781.18	6,200,992.27
Water body	65.07	294.58	8,837.27
Shrubs	1,483.92	155.21	129,130.68
Ricefield	87.52	77.41	3870.75
Mixed dryland farming	2,14	138,28	138,28
Total carbon stock			11,850,478.2

Based on Table 5, the total carbon stock in Pante Ceureumen Protected Forest in 2025 was recorded at 9,307,288.08. This value reflects a significant decline in carbon storage capacity compared to previous conditions, indicating spatial and temporal changes in land cover composition.

Table 5. Carbon stock changes according to land use in 2025

2025			
Land Use and Land Cover	Area	Carbon Density	Total (Mg C)
Primary dryland forest	11,544.52	620.94	4,026,169.72
Secondary dryland forest	12,510.37	464.02	3,257,408.05
Open land	2.56	118.12	1,181.24
Waterbody	287.80	281.01	47,491.05
Mixed dryland farming	2,721.58	376.36	577,704.90
Plantation	1,287.46	266.21	185,019.10
Shrubs	5,280.13	359.66	1,053,090.04
Dryland agriculture	1,148.56	204.92	134,016.95
Settlement	88.34	145.13	5,224.53
Ricefield	88.34	151.62	18,801.25
Mine	43.43	118.12	2,362.48
Total carbon stock			9,307,288.08

Structurally, the primary and secondary dryland forest land cover classes remain the main contributors to carbon stocks, with values reaching up to 4,026,169.72 and 3,257,408.05, respectively. However, these two predominant classes have declined in terms of both total area and carbon contribution, indicating forest ecosystem degradation.

In addition, there was an increase in non-forest land-use classes such as mixed dryland agriculture, plantations, shrubland, settlements, and mining, which generally have lower carbon stock values. For example, the shrubland class has a total carbon stock of 1,053,090.04, while mixed dryland agriculture has 577,704.897. Although their aggregate contribution is quite significant, these values remain lower than those of the forest class, and thus cannot offset the carbon loss resulting from reduced forest cover. This situation indicates a land-use conversion from high-carbon forest ecosystems to land uses with lower carbon stocks, which directly contributes to the decline in total carbon stocks.

These differences in carbon stocks over time indicate that carbon stocks are not uniformly distributed, but are influenced by the heterogeneity of vegetation biomass and uncertainties in spatial carbon mapping [31].

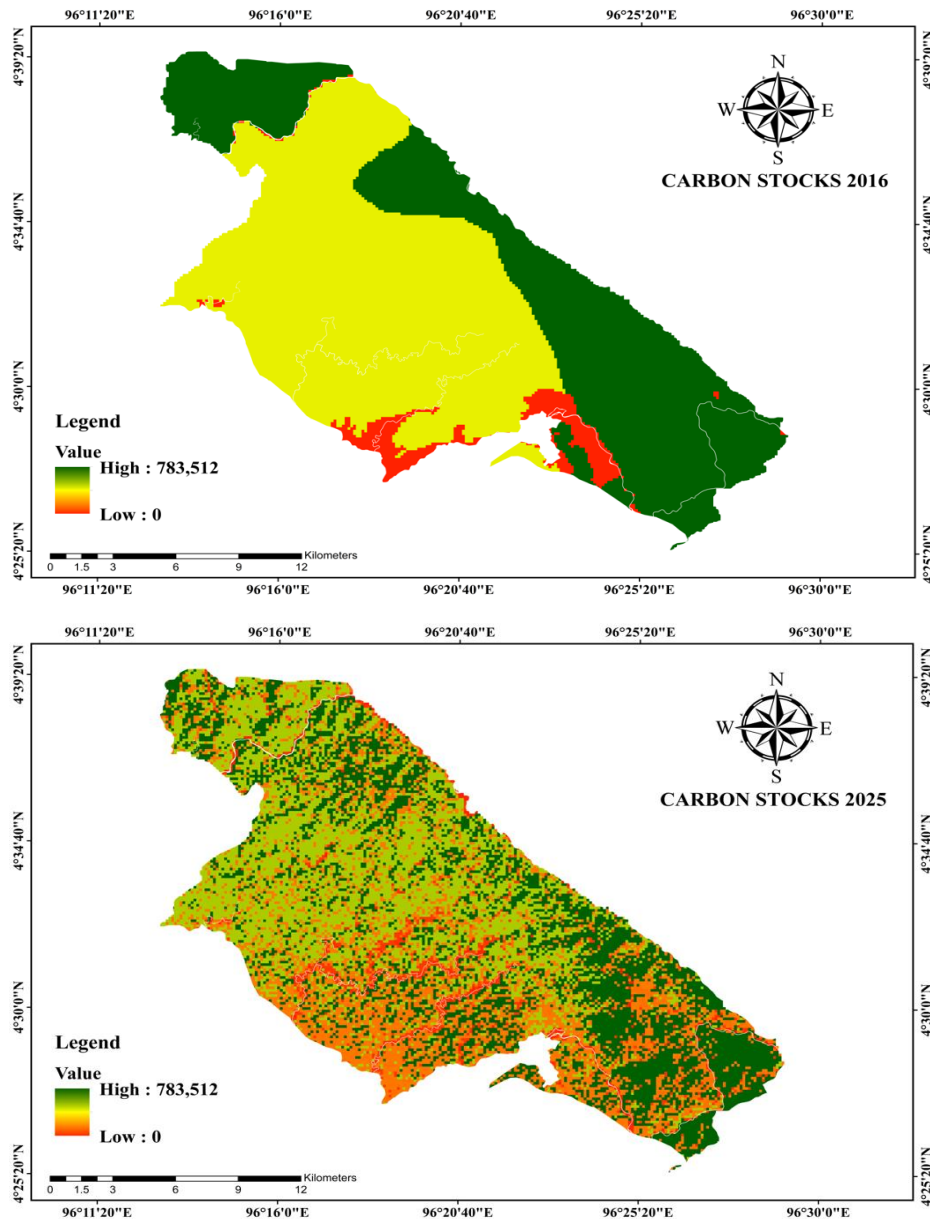
According to the results shown in Tables 4, 5, and 6, the

summary of total carbon stock change calculation using the InVEST model on the 2016-2025 period is shown.

Table 6. Carbon stock result according to the InVEST model

Type	Total Calculation	Units
Total carbon calculation based on 2016 map	11,850,478.2	Mg of C
Total current carbon in 2025	9,307,288.08	Mg of C
Carbon deficit	-2,543,190.12	Mg of C

Based on Table 6, the results of carbon stock modeling using InVEST show that the total carbon stock in the base year 2016 was 11,850,478.2 Mg C, while in the 2025 scenario it was 9,307,288.08 Mg C. Thus, there was a change in carbon stock of -2,543,190.12 Mg C. The map distribution and dynamics change of carbon stocks from 2016 to 2025 is presented in Figure 4. Conceptually, the InVEST model calculates carbon stock based on the carbon density values for each land use and land cover class multiplied by the area, so that changes in land cover composition will directly affect the total carbon stock of a region.



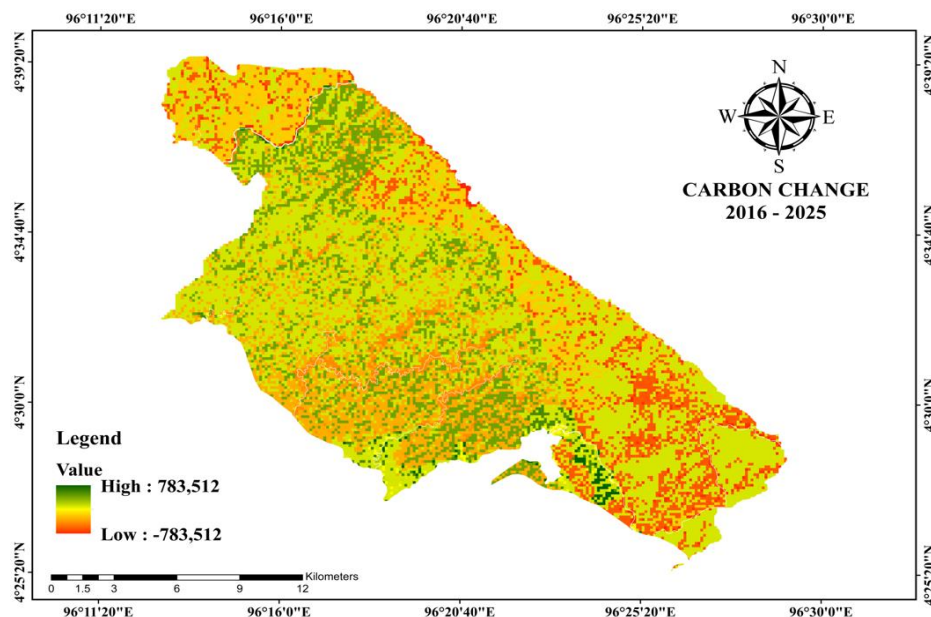


Figure 4. Distribution and dynamics change map of carbon stocking from 2016 to 2025

The decrease in carbon stock in this study can be interpreted as the result of land cover changes, particularly the conversion of high-vegetation classes—such as primary dryland forests and secondary dryland forests—into classes with low carbon stocks, such as mining areas, settlements, and open land. These changes result in a significant reduction in vegetation biomass, thereby decreasing carbon storage capacity in both above-ground and below-ground components. This study aligns with findings that land-use changes, particularly the conversion of forests to other land uses, can lead to a decline in carbon stocks due to the reduction of vegetation that acts as a carbon sink [32].

The decline in carbon stocks in the Pante Ceureumen Protected Forest area is influenced not only by changes in land cover extent but also by the gradual process of forest degradation. Forest degradation occurs when a forest area is still administratively classified as forest but experiences a decline in vegetation quality, canopy density, and biomass due to human activities such as the clearing of access roads, logging, illegal mining, and the expansion of agriculture and plantations. These conditions cause the forest's ability to store carbon to decline, even though some areas still appear forested in satellite imagery. The increase in shrubland area from 1,483.92 ha in 2016 to 5,280.13 ha in 2025 indicates significant forest degradation and landscape fragmentation. The conversion of primary and secondary forests into secondary vegetation with lower biomass results in the loss of large amounts of carbon stocks, as forest classes possess carbon densities far higher than those of shrubland or cultivated land. Deforestation and the reduction in forest area are the primary factors contributing to increased carbon emissions, particularly in developing countries [33].

Temporally, the results of image interpretation indicate that land cover changes tended to increase toward the end of the observation period, particularly around 2016–2025. During this period, a broader and more fragmented increase in non-forest areas began to emerge, particularly in the categories of shrubland, dryland agriculture mixed with shrubs, plantations, and mining. If this trend in land-use change continues without sustainable management, the decline in carbon stocks within the Pante Ceureumen Protected Forest is projected to continue

accelerating in the future.

Forest ecosystems contain approximately 80% of terrestrial carbon above ground and about 40% in the form of soil organic carbon. If these forests are converted into plantations, farm or agricultural land, and settlements, the amount of stored carbon will decline due to changes in the composition of terrestrial biomass [34]. Land use changes significantly influence carbon stock dynamics. The conversion of forest to non-forest land uses leads to a decline in overall carbon stocks [35].

Mitigation strategies to curb the decline in carbon stocks in the Pante Ceureumen Protected Forest can be implemented through the restoration of degraded areas, particularly those where forests have been converted into scrubland, open land, mixed-use agriculture, and mining sites. These efforts include reforestation using native species, rehabilitation of former mining sites, and control of illegal land clearing. Improving the accuracy of Sentinel-2 image classification can also be achieved cost-effectively using ArcGIS by adding training samples, integrating ground check points, and correcting visual interpretations using high-resolution image basemaps, thereby enhancing mapping precision without the need for comprehensive field surveys.

The implementation of carbon restoration policies in protected forest areas still faces various socio-economic challenges. Community dependence on agricultural, plantation, and mining activities is one factor that can hinder forest rehabilitation efforts and land-use conversion control. Additionally, weak law enforcement against illegal activities further increases pressure on forest areas. Therefore, mitigation strategies need to be integrated with community empowerment approaches, sustainable economic development, and increased local community participation in the management of protected forest areas.

Based on the research findings, sustainable land-use policies in the Pante Ceureumen Protected Forest area should focus on restricting the conversion of primary and secondary forests, designating priority rehabilitation zones in degraded areas, and strengthening a system for periodically monitoring land-cover changes using remote sensing. In addition, the implementation of agroforestry practices and conservation-based land use should be developed as land-use alternatives

that continue to support community economic activities without increasing forest degradation and carbon stock depletion.

4. CONCLUSION

InVEST modeling results show that total carbon stocks decreased from 11,850,478.20 Mg C in 2016 to 9,307,288.08 Mg C in 2025, representing a decrease of 2,543,190.12 Mg C. This decline is primarily driven by the conversion of high-biomass forests into non-forest land uses classification with lower carbon density. The research findings underscore the importance of sustainable land management policies through strengthened law enforcement in protected forest areas, rehabilitation of degraded areas, control of illegal mining activities, and the implementation of a periodic remote sensing-based land cover monitoring system to support climate change mitigation and tropical forest carbon conservation.

REFERENCES

[1] Lawler, J.J., Lewis, D.J., Nelson, E., Plantinga, A.J., Polasky, S., Withey, J.C., Helmers, D.P., Martinuzzi, S., Pennington, D., Radeloff, V.C. (2014). Projected land-use change impacts on ecosystem services in the United States. *Proceedings of the National Academy of Sciences*, 111(20): 7492-7497. <https://doi.org/10.1073/pnas.1405557111>

[2] He, C., Zhang, D., Huang, Q., Zhao, Y. (2016). Assessing the potential impacts of urban expansion on regional carbon storage by linking the LUSD-urban and InVEST models. *Environmental Modelling & Software*, 75: 44-58. <https://doi.org/10.1016/j.envsoft.2015.09.015>

[3] Nelson, E.J., Daily, G.C. (2010). Modelling ecosystem services in terrestrial systems. *F1000 Biology Reports*, 2(1): 53. <https://doi.org/10.3410/B2-53>

[4] Eigenbrod, F., Bell, V.A., Davies, H.N., Heinemeyer, A., Armsworth, P.R., Gaston, K.J. (2011). The impact of projected increases in urbanization on ecosystem services. *Proceedings of the Royal Society B*, 278(1722): 3201-3208. <https://doi.org/10.1098/rspb.2010.2754>

[5] IPCC. (2000). *The Intergovernmental Panel on Climate Change, Special Report on Land Use, Land-Use Change, and Forestry*. Cambridge University Press, Cambridge. <https://www.ipcc.ch/report/land-use-land-use-change-and-forestry/>.

[6] Houghton, R.A. (2003). Revised estimates of the annual net flux of carbon to the atmosphere from changes in land use and land management 1850-2000. *Tellus B: Chemical and Physical Meteorology*, 55(2): 378-390. <https://doi.org/10.3402/tellusb.v55i2.16764>

[7] Houghton, R.A., House, J.I., Pongratz, J., van der Werf, G.R., DeFries, R.S., Hansen, M.C., Le Quéré, C., Ramankutty, N. (2012). Carbon emissions from land use and land-cover change. *Biogeosciences*, 9(12): 5125-5142. <https://doi.org/10.5194/bg-9-5125-2012>

[8] Le Quéré, C., Moriarty, R., Andrew, R.M., Peters, G.P., et al. (2015). Global carbon budget 2014. *Earth System Science Data*, 7(1): 47-85. <https://doi.org/10.5194/essd-7-47-2015>

[9] Li, W., Ciaias, P., Peng, S., Yue, C., et al. (2017). Land-

use and land-cover change carbon emissions between 1901 and 2012 constrained by biomass observations. *Biogeosciences*, 14(22): 5053-5067. <https://doi.org/10.5194/bg-14-5053-2017>

[10] Qadeer, A., Shakir, M., Wang, L., Talha, S.M. (2024). Evaluating machine learning approaches for aboveground biomass prediction in fragmented high-elevated forests using multi-sensor satellite data. *Remote Sensing Applications: Society and Environment*, 36: 101291. <https://doi.org/10.1016/j.rsase.2024.101291>

[11] Taddese, H., Asrat, Z., Burud, I., Gobakken, T., Ørka, H.O., Dick, Ø.B., Næsset, E. (2020). Use of remotely sensed data to enhance estimation of aboveground biomass for the dry afro-montane forest in South-Central Ethiopia. *Remote Sensing*, 12(20): 3335. <https://doi.org/10.3390/rs12203335>

[12] Mngadi, M., Odindi, J., Mutanga, O. (2021). The utility of Sentinel-2 spectral data in quantifying above-ground carbon stock in an urban reforested landscape. *Remote Sensing*, 13(21): 4281. <https://doi.org/10.3390/rs13214281>

[13] Guan, D., Nie, J., Zhou, L., Chang, Q., Cao, J. (2023). How to simulate carbon sequestration potential of forest vegetation? *Remote Sensing*, 15(21): 5096. <https://doi.org/10.3390/rs15215096>

[14] Sannigrahi, S. (2017). Modeling terrestrial ecosystem productivity of an estuarine ecosystem in the Sundarban Biosphere Region, India using seven ecosystem models. *Ecological Modelling*, 356: 73-90. <https://doi.org/10.1016/j.ecolmodel.2017.03.003>

[15] Niu, Z., He, H., Peng, S., Ren, X., Zhang, L., Gu, F., Zhu, G., Peng, C., Li, P., Wang, J., Ge, R., Zeng, N., Zhu, X., Lv, Y., Chang, Q., Xu, Q., Zhang, M., Liu, W. (2021). A process-based model integrating remote sensing data for evaluating ecosystem services. *Journal of Advances in Modeling Earth Systems*, 13(6): e2020MS002451. <https://doi.org/10.1029/2020MS002451>

[16] Nel, L., Boeni, A.F., Prohászka, V.J., Szilágyi, A., Tormáné Kovács, E., Pásztor, L., Centeri, C. (2022). InVEST soil carbon stock modelling of agricultural landscapes as an ecosystem service indicator. *Sustainability*, 14(16): 9808. <https://doi.org/10.3390/su14169808>

[17] Hamel, P., Chaplin-Kramer, R., Sim, S., Mueller, C. (2015). A new approach to modeling the sediment retention service (InVEST 3.0): Case study of the cape fear catchment, North Carolina, USA. *Science of the Total Environment*, 524: 166-177. <https://doi.org/10.1016/j.scitotenv.2015.04.027>

[18] Liu, G., Zhao, Z. (2018). Analysis of carbon storage and its contributing factors—A case study in the Loess Plateau (China). *Energies*, 11(6): 1596. <https://doi.org/10.3390/en11061596>

[19] Tang, H., Liu, X., Xie, R., Lin, Y., Fang, J., Yuan, J. (2024). Response of carbon energy storage to land use/Cover changes in Shanxi province, China. *Energies*, 17(13): 3284. <https://doi.org/10.3390/en17133284>

[20] The Natural Capital Project. (2020). *InVEST: Integrated Valuation of Ecosystem Services and Tradeoffs*.

[21] Huang, L., Zhou, M., Lv, J., Chen, K. (2020). Trends in global research in forest carbon sequestration: A bibliometric analysis. *Journal of Cleaner Production*, 252: 119908. <https://doi.org/10.1016/j.jclepro.2019.119908>

[22] Congalton, R.G., Green, K. (2019). Assessing the

- Accuracy of Remotely Sensed Data: Principles and Practices. CRC Press. <https://doi.org/10.1201/9780429052729>
- [23] Wang, S., Zhou, S., Fang, C. (2024). Spatial-temporal patterns and evolution of carbon storage in China's terrestrial ecosystems from 1980 to 2020. *Science China Earth Sciences*, 67: 3270-3287. <https://doi.org/10.1007/s11430-023-1385-9>
- [24] IPCC. (2006). 2006 IPCC guidelines for national greenhouse gas inventories. <https://www.ipcc-nggip.iges.or.jp/public/2006gl/>.
- [25] Sahana, M., Hong, H., Sajjad, H., Liu, J., Zhu, A.X. (2018). Assessing deforestation susceptibility to forest ecosystem in Rudraprayag district, India using fragmentation approach and frequency ratio model. *Science of the Total Environment*, 627: 1264-1275. <https://doi.org/10.1016/j.scitotenv.2018.01.290>
- [26] Nayak, D., Shukla, A.K., Devi, N.R. (2024). Decadal changes in land use and land cover: Impacts and their influence on urban ecosystem services. *AQUA—Water Infrastructure, Ecosystems and Society*, 73(1): 57-72. <https://doi.org/10.2166/aqua.2024.211>
- [27] Kim, D.H., Sexton, J.O., Noojipady, P., Huang, C., Anand, A., Channan, S., Feng, M., Townshend, J.R. (2014). Global, Landsat-based forest-cover change from 1990 to 2000. *Remote Sensing of Environment*, 155: 178-193. <https://doi.org/10.1016/j.rse.2014.08.017>
- [28] Hou, H., Zhang, S., Ding, Z., Huang, A., Tian, Y. (2015). Spatiotemporal dynamics of carbon storage in terrestrial ecosystem vegetation in the Xuzhou coal mining area, China. *Environmental Earth Sciences*, 74(2): 1657-1669. <https://doi.org/10.1007/s12665-015-4171-7>
- [29] Jiao, Y., Wang, Y., Tu, C., Hou, X., Lyu, C., Fan, X., Xia, L. (2024). Spatiotemporal evolution and future of carbon storage in resource-based Chinese province: A case study from Shanxi using PLUS–InVEST model prediction. *Sustainability*, 16(11): 4461. <https://doi.org/10.3390/su16114461>
- [30] Viera, A.J., Garrett, J.M. (2005). Understanding interobserver agreement: The kappa statistic. *Family Medicine*, 37(5): 360-363.
- [31] Mitchard, E.T.A., Saatchi, S.S., Baccini, A., Asner, G.P., Goetz, S.J., Harris, N.L., Brown, S. (2013). Uncertainty in the spatial distribution of tropical forest biomass: A comparison of pan-tropical maps. *Carbon Balance and Management*, 8(1): 10. <https://doi.org/10.1186/1750-0680-8-10>
- [32] Kurniawati, U.F. (2021). Dampak perubahan penggunaan lahan terhadap besaran stok karbon di Kota Surabaya. *Jurnal Penataan Ruang*, 16(1): 54-58. <http://doi.org/10.12962/j2716179X.v16i1.8951>
- [33] Young, O.R. (2010). Institutional dynamics: Resilience, vulnerability and adaptation in environmental and resource regimes. *Global Environmental Change*, 20(3): 378-385. <https://doi.org/10.1016/j.gloenvcha.2009.10.001>
- [34] Hairiah, K., dan Rahayu, S. (2007). Pengukuran Karbon Tersimpan di Berbagai Macam Penggunaan Lahan (p. 110). World Agroforestry Centre.
- [35] Achmad, A., Ramli, I., Sugiarto, S., Irzaidi, I., Izzaty, A. (2024). Assessing and forecasting carbon stock variations in response to land use and land cover changes in Central Aceh, Indonesia. *International Journal of Design & Nature and Ecodynamics*, 19(2): 465-475. <https://doi.org/10.18280/ijdne.190212>